

# Diacylglycerol Kinase $\delta$ Phosphorylates Phosphatidylcholine-specific Phospholipase C-dependent, Palmitic Acid-containing Diacylglycerol Species in Response to High Glucose Levels\*

Received for publication, June 20, 2014, and in revised form, August 8, 2014. Published, JBC Papers in Press, August 11, 2014, DOI 10.1074/jbc.M114.590950

Hiromichi Sakai<sup>‡</sup>, Sayaka Kado<sup>§</sup>, Akinobu Taketomi<sup>¶</sup>, and Fumio Sakane<sup>‡1</sup>

From the <sup>‡</sup>Department of Chemistry, Graduate School of Science and <sup>§</sup>Center for Analytical Instrumentation, Chiba University, 1-33 Yayoi-cho, Inage-ku, Chiba 263-8522 and the <sup>¶</sup>Department of General Surgery, Graduate School of Medicine, Hokkaido University, North 15, West 7, Kita-ku, Sapporo 060-8638, Japan

**Background:** Diacylglycerol (DG) kinase (DGK)  $\delta$  is activated by acute high glucose stimulation.

**Results:** DGK $\delta$  high glucose-dependently phosphorylates 30:0-, 32:0-, and 34:0-DG and interacts with phosphatidylcholine-specific phospholipase C (PC-PLC).

**Conclusion:** DGK $\delta$  utilizes palmitic acid-containing DG species and metabolically connects with PC-PLC.

**Significance:** The newly identified PC-PLC/DGK $\delta$  pathway could play an important role in insulin signaling and glucose uptake.

Decreased expression of diacylglycerol (DG) kinase (DGK)  $\delta$  in skeletal muscles is closely related to the pathogenesis of type 2 diabetes. To identify DG species that are phosphorylated by DGK $\delta$  in response to high glucose stimulation, we investigated high glucose-dependent changes in phosphatidic acid (PA) molecular species in mouse C2C12 myoblasts using a newly established liquid chromatography/MS method. We found that the suppression of DGK $\delta$ 2 expression by DGK $\delta$ -specific siRNAs significantly inhibited glucose-dependent increases in 30:0-, 32:0-, and 34:0-PA and moderately attenuated 30:1-, 32:1-, and 34:1-PA. Moreover, overexpression of DGK $\delta$ 2 also enhanced the production of these PA species. MS/MS analysis revealed that these PA species commonly contain palmitic acid (16:0). D609, an inhibitor of phosphatidylcholine-specific phospholipase C (PC-PLC), significantly inhibited the glucose-stimulated production of the palmitic acid-containing PA species. Moreover, PC-PLC was co-immunoprecipitated with DGK $\delta$ 2. These results strongly suggest that DGK $\delta$  preferably metabolizes palmitic acid-containing DG species supplied from the PC-PLC pathway, but not arachidonic acid (20:4)-containing DG species derived from the phosphatidylinositol turnover, in response to high glucose levels.

Type 2 diabetes is expected to afflict over 300 million people worldwide by 2015 (1). The characteristic features of type 2 diabetes include insulin resistance, glucose intolerance, hyper-

glycemia, and often, hyperinsulinemia (2). Glucose-induced insulin resistance is associated with a temporal increase in the intracellular diacylglycerol (DG)<sup>2</sup> mass in skeletal muscle (3).

DG is metabolized, at least in part, by DG kinase (DGK), which phosphorylates DG to generate phosphatidic acid (PA) (4–8). To date, 10 mammalian DGK isozymes ( $\alpha$ ,  $\beta$ ,  $\gamma$ ,  $\delta$ ,  $\eta$ ,  $\kappa$ ,  $\epsilon$ ,  $\zeta$ ,  $\iota$ , and  $\theta$ ) have been identified, and these isozymes are subdivided into five groups according to their structural features (6, 7). Type II DGKs consist of the  $\delta$ ,  $\eta$ , and  $\kappa$  isoforms (9, 10). Moreover, alternatively spliced forms of DGK $\delta$  ( $\delta$ 1 and  $\delta$ 2) (11) and  $\eta$  ( $\eta$ 1 and  $\eta$ 2) (12) have been found.

DGK $\delta$  is highly expressed in skeletal muscle (13), which is a major insulin-target organ for glucose disposal (14). Chibalin *et al.* (15) demonstrated that DGK $\delta$  regulates glucose uptake and that a decrease in DGK $\delta$  expression resulted in the aggravation of type 2 diabetes. Long term exposure (96 h) to high glucose medium decreased DGK $\delta$  protein levels in primary cultured skeletal muscle cells, and the transcription of DGK $\delta$  and the levels of DGK $\delta$  protein were also reduced in skeletal muscles from type 2 diabetes patients (15). Moreover, DGK $\delta$  haploinsufficient mice (DGK $\delta$ <sup>+/-</sup>) exhibited decreased total DGK activity, reduced DGK $\delta$  protein levels, and the accumulation of DG in skeletal muscle. The increase in the amount of DG caused the increase in the phosphorylation of protein kinase C (PKC)  $\delta$  and a reduction in the expression of the insulin receptor and insulin receptor substrate-1 proteins involved in insulin signaling (15). Furthermore, Miele *et al.* (16) reported that acute high glucose exposure (within 5 min) increased DGK $\delta$  activity in skeletal muscle cells followed by a reduction of PKC $\alpha$  activity and transactivation of the insulin receptor signal.

\* This work was supported in part by grants from the Ministry of Education, Culture, Sports, Science and Technology of Japan; the Japan Science and Technology Agency; the Naito Foundation; the Hamaguchi Foundation for the Advancement of Biochemistry; the Daiichi-Sankyo Foundation of Life Science; the Terumo Life Science Foundation; the Futaba Electronic Memorial Foundation; the Daiwa Securities Health Foundation; the Ono Medical Research Foundation; the Japan Foundation for Applied Enzymology; and the Food Science Institute Foundation.

<sup>1</sup> To whom correspondence should be addressed. Tel./Fax: 81-43-290-3695; E-mail: sakane@faculty.chiba-u.jp.

<sup>2</sup> The abbreviations used are: DG, diacylglycerol; DGK, DG kinase; D609, O-tricyclo[5.2.1.0<sup>2,6</sup>]dec-9-yl dithiocarbonate; FIPI, 5-fluoro-2-indolyl des-chlorohalopemide; ESI, electrospray ionization; PA, phosphatidic acid; PC, phosphatidylcholine; PC-PLC, PC-specific phospholipase C; PLD, phospholipase D; TOFA, 5-(tetradecyloxy)-2-furoic acid; PI, phosphatidylinositol; DMSO, dimethyl sulfoxide; AcGFP, GFP from *Aequorea coerulescens*.

## Metabolic Linkage between PC-PLC and DGK $\delta$

Hence, these studies indicate that DG consumed by DGK $\delta$  in response to high glucose exposure is a key regulator of glucose uptake in skeletal muscle cells. DGK $\delta$ 1 translocated from the cytoplasm to the plasma membrane in mouse myoblast C2C12 cells within 5 min of short term exposure to a high glucose concentration, whereas DGK $\delta$ 2 was located in punctate vesicles irrespective of the glucose concentration (17).

Mammalian cells contain at least 50 structurally distinct molecular DG species because DG contains a variety of fatty acyl moieties at positions 1 and 2 (18). In general, DGs containing arachidonic acid (20:4), especially 18:0/20:4-DG (38:4-DG), in the phosphatidylinositol (PI) turnover are important molecules that serve as second messengers for PKC activation (18). Moreover, previous studies have demonstrated that DGK $\epsilon$  preferably phosphorylates arachidonic acid-containing DGs derived from PI turnover (19, 20). Therefore, it is generally believed that all DGKs preferentially metabolize 38:4-DG for the regulation of signal transduction. However, the DG molecular species phosphorylated by DGK $\delta$  in response to glucose stimulation remain unknown.

In this study, we investigated the changes in the amounts of PA molecular species that are produced by DGK in glucose-stimulated C2C12 myoblasts using our previously developed liquid chromatography/electrospray ionization mass spectrometry (LC/ESI-MS) method (21) to identify the DG molecular species metabolized by DGK $\delta$  under short term high glucose conditions. Interestingly, the LC/ESI-MS analyses indicated that DGK $\delta$  preferably metabolizes limited DG molecular species, 30:0-, 30:1-, 32:0-, 32:1-, 34:0-, and 34:1-DG, commonly containing palmitic acid (16:0), but not DG species containing arachidonic acid in response to high glucose stimulation. Moreover, the 30:0-, 32:0-, and 34:0-DG species were suggested to be supplied by phospholipase C (PLC)-dependent phosphatidylcholine (PC) hydrolysis, indicating an unexpected linkage between PC-PLC and DGK $\delta$ .

### EXPERIMENTAL PROCEDURES

**Cell Culture**—C2C12 mouse myoblasts were maintained on 100-mm dishes in DMEM (Wako Pure Chemicals) containing 10% FBS (Biological Industries-Invitrogen) at 37 °C in an atmosphere containing 5% CO<sub>2</sub>. For differentiation to myotubes, confluent C2C12 myoblasts were cultured in differentiation medium (DMEM containing 0.1% FBS and 5  $\mu$ g/ml insulin (Sigma-Aldrich)) for 4 days.

**Establishment of a Stable Cell Line Overexpressing DGK $\delta$** —To establish C2C12 cells stably expressing human DGK $\delta$ 2, the cells were transfected with pAcGFP-DGK $\delta$ 2 (11, 17) using PolyFect (Qiagen) according to the instruction manual and were selected with 800  $\mu$ g/ml G418 for 2 weeks. Single colonies were isolated and then were then grown in DMEM containing 10% FBS.

**RNA Interference**—To silence the expression of mouse DGK $\delta$ , the following Stealth RNAi duplexes (Invitrogen) were used: DGK $\delta$ -siRNA-1, 5'-GAAUGUGAUGCUGGAUCUUAC-UAAA-3' and 5'-UUUAGUAAGAUCAGCAUCACAUUC-3'; DGK $\delta$ -siRNA-2, 5'-UGGCAUUGGCUUGGAUGCAAAGUAU-3' and 5'-UAUCUUUGCAUCCAAGCCAAUGCCA-3'. The duplexes were transfected into C2C12 myoblasts by electropor-

ation (at 350 V and 300 microfarads) using the Gene Pulser Xcell™ electroporation system (Bio-Rad Laboratories). The transfected cells were then allowed to grow for 48 h in DMEM containing 10% FBS.

**Glucose Stimulation and Treatment with Lipid Metabolism Enzyme Inhibitors**—Glucose stimulation was performed as reported previously (16). Briefly, untransfected C2C12 myoblasts and C2C12 myoblasts transfected with Stealth RNAi duplexes were grown on poly-L-lysine (Sigma-Aldrich)-coated culture dishes. The cells were rinsed and incubated in glucose-free medium (16) in the absence or presence of PC-PLC inhibitor *O*-tricyclo[5.2.1.0<sup>2,6</sup>]dec-9-yl dithiocarbonate (D609, 100  $\mu$ M, Calbiochem) (22), acetyl-CoA carboxylase inhibitor 5-(tetradecyloxy)-2-furoic acid (TOFA, 20  $\mu$ M, Calbiochem) (23, 24), or phospholipase D (PLD) inhibitor 5-fluoro-2-indolyl deschlorohalopemide (FIPI, 100 nM, Calbiochem) (25) for 3 h. The cells were incubated for 5 min in the same buffer supplemented with 25 mM glucose.

**Lipid Extraction and Western Blot Analysis**—The cells grown under each culture condition were harvested and lysed in ice-cold lysis buffer (50 mM HEPES, pH 7.2, 150 mM NaCl, 5 mM MgCl<sub>2</sub>, 1 mM dithiothreitol, cOmplete™ EDTA-free protease inhibitor (Roche Diagnostics)) followed by centrifugation at 1,000  $\times$  *g* for 5 min at 4 °C. Total lipids were extracted from the cell lysates (1.0 mg of protein), in which DGK $\delta$  expression was confirmed by Western blot analysis using an anti-DGK $\delta$  antibody (13), according to the method of Bligh and Dyer (26). The extracted lipids were used for subsequent MS analyses.

**Analysis of PA Molecular Species**—PAs in extracted cellular lipids (5  $\mu$ l) containing 40 pmol of the 14:0/14:0-PA internal standard (Sigma-Aldrich) were analyzed separately by LC/ESI-MS using an Accela LC system (Thermo Fisher Scientific) coupled online to an Exactive Orbitrap MS (Thermo Fisher Scientific) equipped with an ESI source as described previously (21). The MS peaks are presented in the form of *X*:*Y*, where *X* is the total number of carbon atoms and *Y* is the total number of double bonds in both acyl chains of the PA.

For the identification of fatty acid residues in PA molecular species by ESI-MS/MS, PA molecular species (28:0–40:0-PA) were fractionated using the above LC/ESI-MS system equipped with an FC 203B fraction collector (Gilson). The mixture of these isolated PA molecular species was infused into an Exactive Orbitrap MS (Thermo Fisher Scientific) equipped with a syringe pump (an infusion rate of 5  $\mu$ l/min) and an ESI source. A collision energy of 40 eV was used to obtain fragment ions.

**Analysis of DG Molecular Species**—The isolation of DG was performed according to previously reported procedures (27). The extracted cellular lipids (per 1 mg of protein) were developed on Silica Gel 60 high performance thin layer chromatography plates (Merck, 10  $\times$  20 cm) using hexane/diethyl ether/acetic acid (75:25:1, v/v). After development, DG was extracted from silica gel and redissolved in 200  $\mu$ l of methanol:chloroform (9:1, v/v) containing 1  $\mu$ g/ml 12:0/12:0-DG (Avanti Polar Lipids), and 10  $\mu$ l of 100 mM sodium acetate were added to each sample (28). MS analysis was performed on an Exactive Orbitrap MS (Thermo Fisher Scientific) equipped with a Fusion 100T syringe pump (an infusion rate of 5  $\mu$ l/min, Thermo Fisher Scientific) and an ESI source. The ion spray

voltage was set to 5 kV in the positive ion mode. The capillary temperature was set to 300 °C.

**Measurement of DGK $\delta$  Activity**—The octyl glucoside-mixed micellar assay of DGK activity was performed as described previously (12). COS-7 cells transfected with p3 $\times$ FLAG-DGK $\delta$ 2 (29) were harvested and lysed in ice-cold lysis buffer followed by centrifugation at 1,000  $\times$  *g* for 5 min at 4 °C. The cell lysates were added to octyl glucoside buffer containing 2 mM 16:0/16:0-, 16:0/18:1-, or 18:0/20:4-DG (Avanti Polar Lipids) and 10 mM phosphatidylserine (Avanti Polar Lipids).

**Immunoprecipitation and Measurement of PC-PLC Activity**—The glucose-stimulated cells stably expressing human DGK $\delta$ 2 were harvested and lysed in ice-cold lysis buffer (50 mM HEPES, pH 7.2, 150 mM NaCl, 5 mM MgCl<sub>2</sub>, 1% Nonidet P-40, 1 mM dithiothreitol, cOmplete<sup>TM</sup> EDTA-free protease inhibitor (Roche Diagnostics)) for immunoprecipitation. The mixtures were centrifuged at 12,000  $\times$  *g* for 5 min at 4 °C to yield the cell lysates. 500  $\mu$ g of the cell lysates were incubated with normal rabbit IgG (2  $\mu$ g, Santa Cruz Biotechnology) or rabbit anti-DGK $\delta$  antibody (2  $\mu$ g) (13, 29) at 4 °C overnight and incubated with protein A/G PLUS-agarose (Santa Cruz Biotechnology) for an additional 1 h. The bead-bound proteins were washed with ice-cold wash buffer (50 mM HEPES, pH 7.2, 100 mM NaCl, 5 mM MgCl<sub>2</sub>, 0.1% Triton X-100, 10% glycerol, 20 mM NaF) four times and resolved in 70  $\mu$ l of 1 $\times$  reaction buffer (50 mM Tris-HCl, pH 7.4, 140 mM NaCl, 10 mM dimethylglutarate, 2 mM CaCl<sub>2</sub>) in the Amplex Red<sup>®</sup> PC-PLC assay kit (Molecular Probes-Life Technologies). In this enzyme-coupled assay, PC-PLC activity is monitored indirectly using 10-acetyl-3,7-dihydroxyphenoxazine (Amplex Red<sup>®</sup> reagent), a sensitive fluorogenic probe for H<sub>2</sub>O<sub>2</sub>. First, PC-PLC converts PC to form phosphocholine and DG. After the action of alkaline phosphatase, which hydrolyzes phosphocholine, choline is oxidized by choline oxidase to betaine and H<sub>2</sub>O<sub>2</sub>. Finally, H<sub>2</sub>O<sub>2</sub>, in the presence of horseradish peroxidase, reacts with Amplex Red<sup>®</sup> reagent in a 1:1 stoichiometry to generate the highly fluorescent product, resorufin. Resorufin has absorption and fluorescence emission maxima of  $\sim$ 571 nm and 585 nm, respectively. 50- $\mu$ l aliquots of the mixtures were used for the measurement of PC-PLC activities, and 10  $\mu$ l of the mixtures were used for Western blot analysis.

**Statistics**—All LC/ESI-MS data were normalized based on the protein content and the intensity of the internal standard. The data were represented as the mean  $\pm$  S.D. Statistical analysis was performed using the two-tailed *t* test or analysis of variance followed by Tukey's post hoc test.

## RESULTS

**Increase in the Amount of PA by Acute Stimulation with High Glucose**—We first examined whether the amount of total PA was increased in C2C12 myoblasts stimulated with 25 mM glucose. As shown in Fig. 1A, LC/ESI-MS analysis indicated that exposure to high glucose levels (for 5 min) statistically increased the total PA amounts (1.23-fold, *p* < 0.005). In addition, the stimulation significantly increased the amounts of C30 to C36 PA molecular species, with the exception of 36:1-PA (Fig. 1B). However, the stimulation did not substantially affect

the production of C38 to C40 PA molecular species, including 38:4-PA, with the exception of 38:6-PA.

We investigated the high glucose-dependent increases of total PA amount and PA molecular species in C2C12 myoblasts at different time points. After 5 min of glucose stimulation, the levels of total PA and PA molecular species were significantly increased (Fig. 1, C and D). However, total PA and PA molecular species levels returned close to basal levels by prolonging the incubation with high glucose concentrations for up to 15 and 30 min. We confirmed that DGK activity *in vitro* was increased by glucose stimulation for 5 min (data not shown). These results strongly suggest that C2C12 myoblasts and L6 myotubes (16) have essentially the same lipid metabolism pathway to produce PA in response to acute glucose stimulation.

We confirmed the changes in the amounts of PA molecular species in C2C12 myotubes in response to acute high glucose stimulation (5 min). The glucose-stimulated C2C12 myotubes showed essentially the same results (Fig. 1, E and F) as those obtained with C2C12 myoblasts (Fig. 1, A and B). The results support that C2C12 myoblasts and myotubes possess essentially the same lipid metabolism pathway to produce PA in response to high glucose stimulation. Because C2C12 myoblasts were more efficiently transfected with siRNAs than C2C12 myotubes, C2C12 myoblasts were used for identification of PA molecular species produced by DGK $\delta$  in response to high glucose stimulation.

**Effects of DGK $\delta$ -specific siRNAs on High Glucose-induced Increases in PA Molecular Species**—To clarify whether the glucose-stimulated production of PA molecular species is catalyzed by DGK $\delta$ , we investigated the effects of a DGK $\delta$ -specific siRNA, DGK $\delta$ -siRNA-1. Of the two alternatively spliced DGK $\delta$  products, DGK $\delta$ 1 and DGK $\delta$ 2 (11), C2C12 myoblasts predominantly expressed DGK $\delta$ 2 (Fig. 2A). DGK $\delta$ -siRNA-1 efficiently suppressed DGK $\delta$ 2 expression in C2C12 myoblasts (Fig. 2A). To facilitate comparison, averages of the relative values (+glucose *versus* -glucose) from four independent experiments are displayed (Fig. 2B). Interestingly, the suppression of DGK $\delta$  expression by DGK $\delta$ -siRNA-1 significantly inhibited the glucose stimulation-dependent production of saturated fatty acid-containing C30-C34 PA species, 30:0-, 32:0-, and 34:0-PA, to their basal levels. In addition, one saturated and one monounsaturated fatty acid-containing PA, 34:1-PA, decreased as well. However, the amount of arachidonic acid (20:4)-containing PA, 38:4-PA, was not markedly changed (Fig. 2B). To rule out off-target effects of DGK $\delta$ -siRNA-1, we employed an independent siRNA targeted to a different region of DGK $\delta$  mRNA (DGK $\delta$ -siRNA-2). DGK $\delta$ -siRNA-2, which suppressed DGK $\delta$ 2 expression slightly less strongly than DGK $\delta$ -siRNA-1 (Fig. 2C), also statistically inhibited the production of 30:0-, 34:1-, and 34:0-PA and moderately attenuated 32:0-PA generation (Fig. 2D). These results suggest that DGK $\delta$  selectively phosphorylated 30:0-, 32:0-, 34:1-, and 34:0-DG, which contain either two saturated fatty acids or one saturated and one monounsaturated fatty acids, but not 38:4-PA.

We investigated whether the decreases in the amounts of 30:0-, 32:0-, 34:1-, and 34:0-PA by DGK $\delta$ -siRNAs were due to decreases in the substrates, the corresponding DG species, in high glucose-stimulated and -unstimulated C2C12 myoblasts.

## Metabolic Linkage between PC-PLC and DGK $\delta$

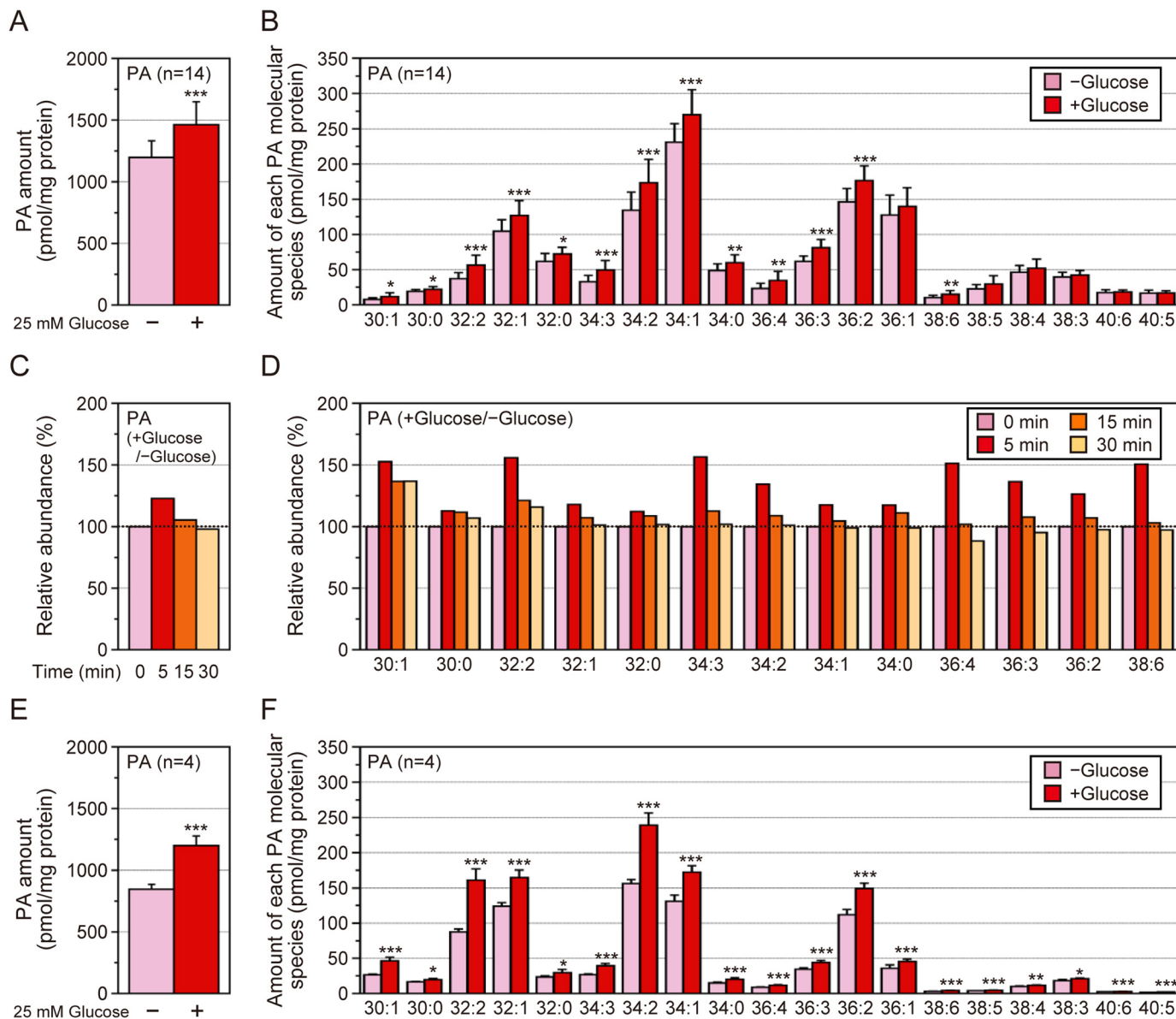


**FIGURE 1. Changes in the total PA and PA molecular species by high glucose stimulation in C2C12 myoblasts and myotubes.** *A* and *B*, the amounts of the total PAs (*A*) and major PA molecular species (*B*) in the glucose-unstimulated or glucose-stimulated C2C12 myoblasts were quantified using the LC/ESI-MS method. The values are presented as the mean  $\pm$  S.D. ( $n = 14$ ). \*,  $p < 0.05$ ; \*\*,  $p < 0.01$ ; \*\*\*,  $p < 0.005$  (no stimulation versus glucose stimulation). *C* and *D*, the amounts of the total PAs (*C*) and major PA molecular species (*D*) that statistically increased in *A* in the cells stimulated by glucose for 5, 15, or 30 min were detected using the LC/ESI-MS method. The results are presented as the percentage of the value of PA molecular species in glucose-unstimulated cells. The values are presented as the mean ( $n = 2$ ). Essentially the same results were obtained in two independent experiments. *E* and *F*, the amounts of the total PAs (*E*) and major PA molecular species (*F*) in the glucose-unstimulated or glucose-stimulated C2C12 myotubes were quantified using the LC/ESI-MS method. The values are presented as the mean  $\pm$  S.D. ( $n = 4$ ). \*,  $p < 0.05$ ; \*\*,  $p < 0.01$ ; \*\*\*,  $p < 0.005$  (no stimulation versus glucose stimulation).

Glucose stimulation substantially increased the amounts of various DG species (Fig. 3). However, DGK $\delta$ -siRNA-1 failed to significantly affect the amounts of 30:0-, 32:0-, 34:1-, and 34:0-DG molecular species both in the absence and in the presence of high glucose levels. Therefore, it is likely that the decreases in the amounts of 30:0-, 32:0-, 34:1-, and 34:0-PA were not caused by decreased amounts of the corresponding DG species.

**Effect of Overexpression of DGK $\delta$  on the Production of PA Molecular Species**—To confirm the results of the siRNA experiments, we evaluated the result of DGK $\delta$ 2 overexpression on high glucose-dependent production of PA species in C2C12 cells. In response to high glucose, the levels of 30:0-, 32:0-, and

34:0-PA statistically increased in C2C12 cells stably expressing DGK $\delta$ 2 when compared with control cells (Fig. 4*B*). Moreover, 30:1- and 32:1-PA were also augmented. In contrast, 38:4-PA did not increase. Taken together with the siRNA results (Figs. 2 and 4), these results support the hypothesis that DGK $\delta$  phosphorylated DG species with an apparent preference for 30:0-, 32:0-, and 34:0-DG, but not arachidonic acid-containing DG, 38:4-DG. Moreover, it is possible that this enzyme also generates 30:1-, 32:1-, and 34:1-PA.

**Fatty Acid Composition of 30:0-, 32:0-, and 34:0-PA**—We next determined the molecular identities of the two fatty acids included in 30:0-, 32:0-, and 34:0-PA, which were indicated to be selectively generated by DGK $\delta$ 2 in C2C12 cells. ESI-MS/MS

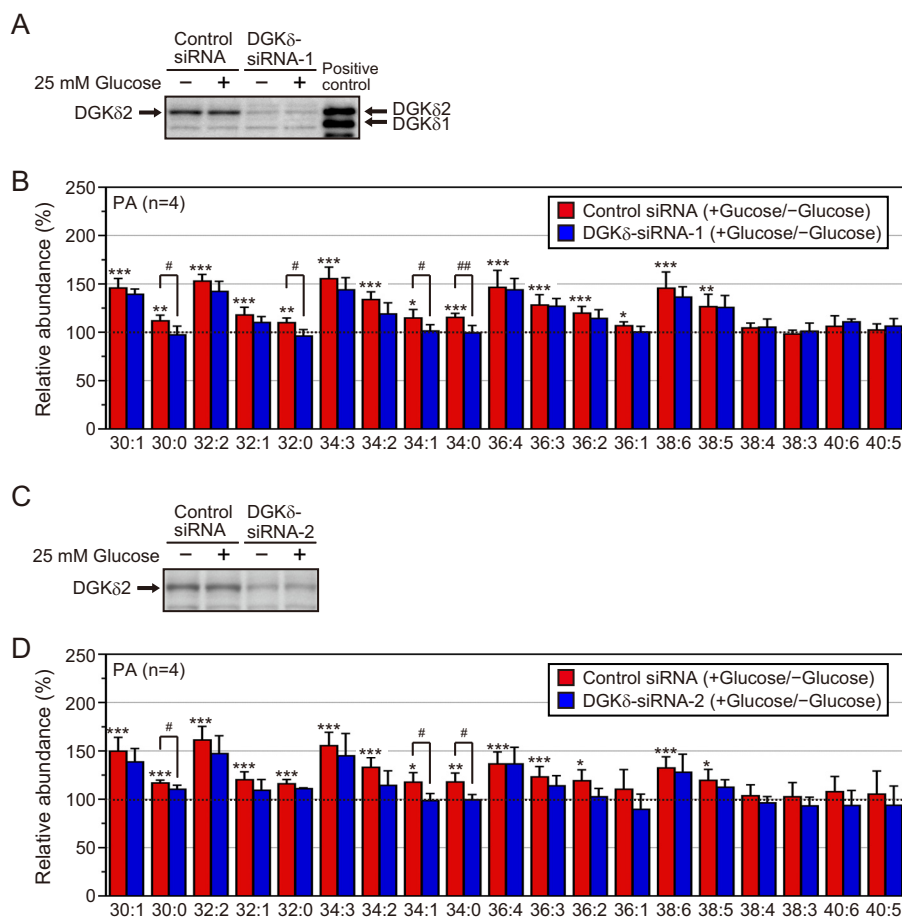


**FIGURE 2. Effects of DGK $\delta$ -siRNA-1 and -2 on high glucose-induced increases of PA molecular species in C2C12 myoblasts.** A and C, the suppression of DGK $\delta$ 2 expression by DGK $\delta$ -siRNA-1 (A) or DGK $\delta$ -siRNA-2 (C) was confirmed by Western blot analysis using the anti-DGK $\delta$  antibody. Human DGK $\delta$ 1 and DGK $\delta$ 2 (11) expressed in COS-7 cells were electrophoresed as a control (A). B and D, the major PA molecular species in the glucose-unstimulated or glucose-stimulated cells transfected with control siRNA or DGK $\delta$ -siRNA-1/2 were detected using the LC/ESI-MS method. The results are presented as the percentage of PA molecular species in glucose-unstimulated cells transfected with control siRNA or DGK $\delta$ -siRNA-1/2. DGK $\delta$ -siRNA-1/2 did not significantly affect the value of PA molecular species in glucose-unstimulated cells. The values are presented as the mean  $\pm$  S.D. ( $n = 4$ ). \*,  $p < 0.05$ ; \*\*,  $p < 0.01$ ; \*\*\*,  $p < 0.005$  (no stimulation versus glucose stimulation). #,  $p < 0.05$ ; ##,  $p < 0.01$  (control siRNA versus DGK $\delta$ -siRNA-1 or DGK $\delta$ -siRNA-2).

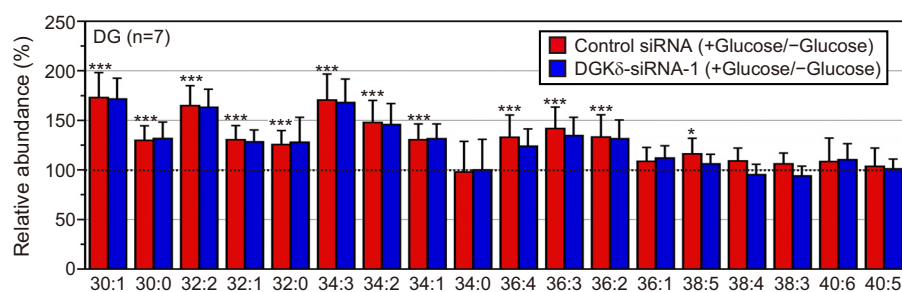


**FIGURE 3. Effect of DGK $\delta$ -siRNA-1 on high glucose-induced increases of DG molecular species in C2C12 myoblasts.** The major DG molecular species in the glucose-unstimulated or glucose-stimulated cells transfected with control siRNA or DGK $\delta$ -siRNA-1 were detected using the ESI-MS method. The results are presented as the percentage of the value of DG molecular species in glucose-unstimulated cells transfected with control siRNA or DGK $\delta$ -siRNA-1. DGK $\delta$ -siRNA-1 did not significantly affect the value of DG molecular species in glucose-unstimulated cells. The values are presented as the mean  $\pm$  S.D. ( $n = 7$ ). \*,  $p < 0.05$ ; \*\*\*,  $p < 0.005$  (no stimulation versus glucose stimulation).

analysis revealed that the main fatty acid residues were as follows: 30:0 consisted of 14:0 and 16:0 (100%), 32:0 included 16:0 and 16:0 (96.6%), and 34:0 contained 16:0 and 18:0 (99.7%) (Table 1). These results indicate that 30:0-, 32:0-, and 34:0-PA consist of relatively short saturated fatty acids and commonly contain palmitic acid (16:0). It is possible that DGK $\delta$ 2 also produces 30:1-, 32:1-, and 34:1-PA species (Figs. 2 and 4). These PA

species contain saturated fatty acids, 16:0 and 14:0, and mono-unsaturated fatty acids, 16:1 and 18:1 (Table 1).

**In Vitro DGK $\delta$  Activity**—We examined whether the preference of DGK $\delta$ 2 for palmitic acid (16:0)-containing DG species, 30:0-, 32:0-, and 34:0-DG, is an intrinsic catalytic feature of DGK $\delta$ . To this end, we measured DGK $\delta$ 2 activity *in vitro* using 32:0 (16:0/16:0)-, 34:1 (16:0/18:1)-, or 38:4 (18:0/20:4)-DG as

## Metabolic Linkage between PC-PLC and DGK $\delta$

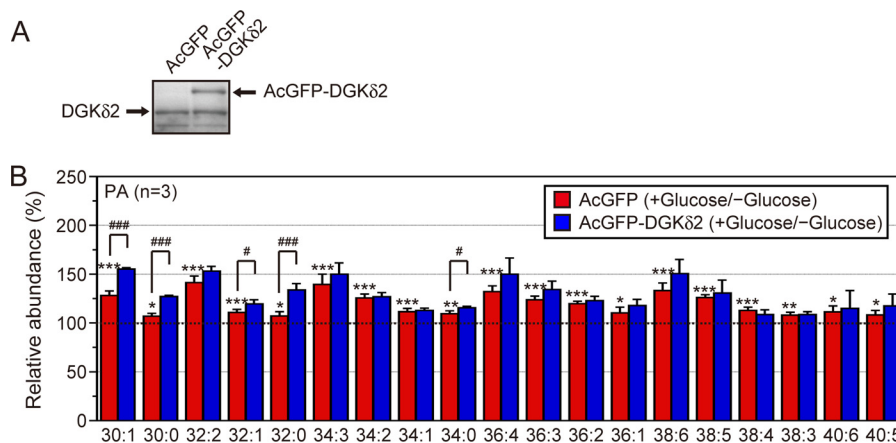


**FIGURE 4. PA molecular species in C2C12 cells stably expressing DGK $\delta$ .** A, the stable expression of AcGFP-DGK $\delta$  in C2C12 cells was confirmed by Western blot analysis using the anti-DGK $\delta$  antibody. B, the major PA molecular species in the glucose-unstimulated or glucose-stimulated cells stably expressing human DGK $\delta$ 2 were identified and quantified using LC/ESI-MS. The results are presented as the percentage of the value of PA molecular species in glucose-unstimulated cells transfected with AcGFP alone or AcGFP-DGK $\delta$ 2. Overexpression of DGK $\delta$ 2 did not significantly affect the value of PA molecular species in glucose-unstimulated cells. The values are presented as the mean  $\pm$  S.D. ( $n = 3$ ). \*,  $p < 0.05$ ; \*\*,  $p < 0.01$ ; \*\*\*,  $p < 0.005$  (no stimulation *versus* glucose stimulation). #,  $p < 0.05$ ; ###,  $p < 0.005$  (no overexpression *versus* DGK $\delta$  overexpression).

**TABLE 1**  
Identification of the acyl species in each PA molecular species

PA molecular species	Identified acyl chains <sup>a</sup>	
30:1	14:0/16:1 (86.0%)	16:0/14:1 (14.0%)
30:0	14:0/16:0 (100%)	
32:2	16:1/16:1 (98.5%)	14:0/18:2 (1.5%)
32:1	16:0/16:1 (88.7%)	14:0/18:1 (11.3%)
32:0	16:0/16:0 (96.6%)	14:0/18:0 (3.4%)
34:3	16:1/18:2 (67.2%)	16:2/18:1 (27.7%)
34:2	16:1/18:1 (86.3%)	16:0/18:2 (13.6%)
34:1	16:0/18:1 (93.2%)	18:0/16:1 (6.8%)
34:0	16:0/18:0 (99.7%)	14:0/20:0 (0.3%)
36:4	16:0/20:4 (83.0%)	16:1/20:3 (8.7%)
36:3	18:1/18:2 (74.9%)	16:0/20:3 (23.6%)
36:2	18:1/18:1 (91.6%)	18:0/18:2 (5.0%)
36:1	18:0/18:1 (87.8%)	16:0/20:1 (6.5%)
38:6	16:0/22:6 (68.0%)	16:1/22:5 (30.9%)
38:5	16:0/22:5 (45.0%)	18:1/20:4 (45.0%)
38:4	18:0/20:4 (80.1%)	18:1/20:3 (19.5%)
38:3	18:0/20:3 (88.6%)	18:1/20:2 (10.5%)
40:6	18:1/22:5 (51.5%)	18:0/22:6 (47.6%)
40:5	18:0/22:5 (97.4%)	18:1/22:4 (2.6%)

<sup>a</sup> The relative abundance (%) was based on the peak areas of the fragment ions (ESI-MS/MS) for each molecular ion.

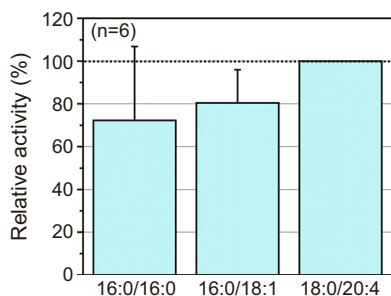


**FIGURE 5. *In vitro* DGK $\delta$  activity.** For measurement of *in vitro* DGK $\delta$  activity, 2 mM (5.4 mol%) 16:0/16:0-, 16:0/18:1-, and 18:0/20:4-DG were used as substrates. The activity of 3 $\times$ FLAG-tagged DGK $\delta$ 2 in COS-7 cells was compared with the control. The results are presented as the percentage of the value of activity against 18:0/20:4-DG. The values are presented as the mean  $\pm$  S.D. ( $n = 6$ ).

substrates. As shown in Fig. 5, the levels of 32:0- and 34:1-PA generated by DGK $\delta$ 2 were similar to or slightly lower than that of 38:4-PA. These results indicate that DGK $\delta$ 2 does not exhibit intrinsic substrate selectivity for particular DG molecular species, 32:0-DG, *in vitro*. Therefore, we hypothesized that DGK $\delta$

accomplishes apparent substrate selectivity in C2C12 cells by accessing a DG pool containing only 30:0-, 32:0-, and 34:0-DG, and not based on the intrinsic properties of the enzyme.

**Effects of Inhibitors of Lipid Metabolism Enzymes on High Glucose Level-induced PA Production**—To test this hypothesis, we next searched for the lipid metabolic pathway that supplies 30:0-, 32:0-, and 34:0-DG species as a substrate for DGK $\delta$ 2. There are three pathways that produce DG, 1) the *de novo* pathway (30, 31), 2) the PLD/PA phosphatase pathway (32), and 3) the PC-specific PLC pathway (33). The treatment with 20  $\mu$ M TOFA, which inhibits acetyl-CoA carboxylase involved in the *de novo* synthesis of DG (23, 24), did not decrease the glucose-stimulated production of PA molecular species (Fig. 6A). Moreover, 100 nM FIPI, which inhibits PLD involved in DG generation from PC through the action of PA phosphatase (25), reduced the amounts of most of the PAs in the absence of high glucose stimulation (data not shown). However, this compound failed to attenuate the glucose-stimulated production of PA molecular species (Fig. 6B). These results strongly suggest that these pathways are not involved in the DG supply to DGK $\delta$ 2.

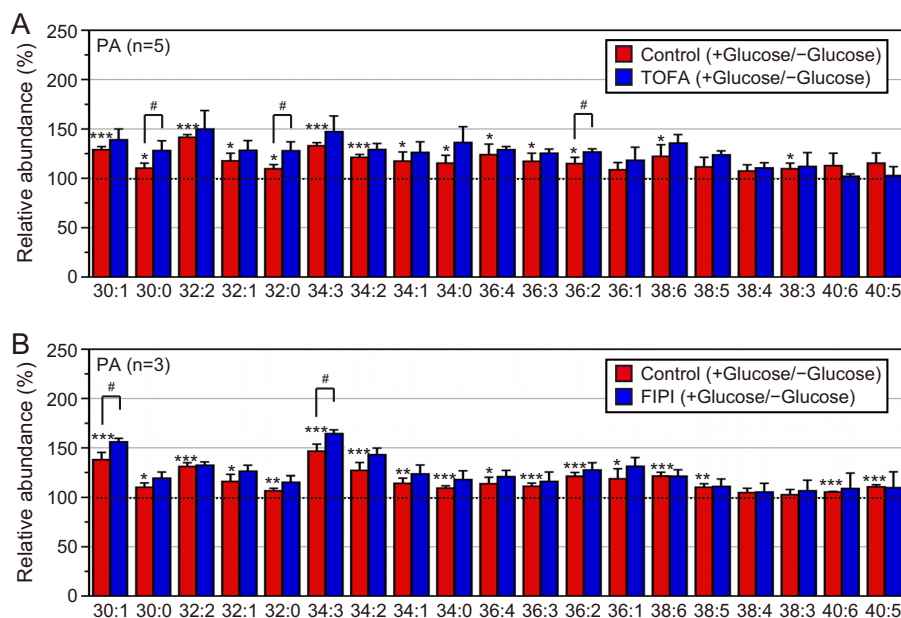


**FIGURE 6. Effects of TOFA and FIPI on the production of PA molecular species in glucose-stimulated C2C12 cells.** A, the major PA molecular species in glucose-unstimulated or glucose-stimulated cells treated with DMSO (control) or TOFA were detected using the LC/ESI-MS method. The results are presented as the percentage of the value of PA species in glucose-unstimulated cells treated with DMSO (control) or TOFA. The values are presented as the mean  $\pm$  S.D. ( $n = 5$ ). \*,  $p < 0.05$ ; \*\*\*,  $p < 0.005$  (no stimulation versus glucose stimulation). #,  $p < 0.05$  (without TOFA versus with TOFA). B, the major PA molecular species in the glucose-unstimulated or glucose-stimulated cells treated with DMSO (control) or FIPI were detected using the LC/ESI-MS method. The results are presented as the percentage of the value of PA species in glucose-unstimulated cells treated with DMSO (control) or FIPI. The values are presented as the mean  $\pm$  S.D. ( $n = 3$ ). \*,  $p < 0.05$ ; \*\*,  $p < 0.01$ ; \*\*\*,  $p < 0.005$  (no stimulation versus glucose stimulation). #,  $p < 0.05$  (without FIPI versus with FIPI).

D609 is an inhibitor of PC-PLC (22), which generates DG via PC hydrolysis (34). Treatment with 100  $\mu$ M D609 strongly inhibited the high glucose stimulation-responsive production of 30:0-, 32:0-, and 34:0-PA to their basal levels (Fig. 7A), suggesting that DGK $\delta$  utilizes DG species supplied from the PC-PLC pathway.

We next confirmed that D609 inhibited the production of DG molecular species, including 30:0-, 32:0-, and 34:0-DG. This inhibitor statistically attenuated the amounts of 30:0-, 32:0-, and 34:0-DG in the absence of high glucose stimulation (Fig. 7B). However, D609 inhibited high glucose-dependent increases for all of the C30-C34 DG species (Fig. 7C). These results suggest that, in response to acute high glucose stimulation (5 min), DGK $\delta$  can utilize DG species that are supplied from the PC-PLC pathway, in both high glucose-independent and high glucose-dependent manners.

**Linkage between PC-PLC and DGK $\delta$** —To further examine the linkage between the PC-PLC pathway and DGK $\delta$ , we determined whether D609 and DGK $\delta$ -siRNA-1 additively affected the high glucose-dependent increases of 30:0-, 32:0-, and 34:0-PA. If DGK $\delta$  utilizes DG species supplied from the PC-PLC pathway, it would be expected that reduced expression of DGK $\delta$  via DGK $\delta$ -siRNA-1 would not enhance the effect of the PC-PLC inhibitor. It was confirmed that the expression of DGK $\delta$  was substantially reduced by DGK $\delta$ -siRNA-1, even in the presence of D609 (Fig. 8A). As shown in Fig. 8B, DGK $\delta$ -siRNA-1 failed to further inhibit the glucose-dependent increases of 30:0-, 32:0-, and 34:0-PA in the presence of D609. These results strongly suggest that 30:0-, 32:0-, and 34:0-DG phosphorylated by DGK $\delta$  in response to acute high glucose exposure are generated, at least in part, by PC hydrolysis catalyzed by PC-PLC.

We next examined whether DGK $\delta$  directly or indirectly interacted with PC-PLC. To this end, we used C2C12 cells stably overexpressing DGK $\delta$ 2 (Fig. 4) and stimulated the cells with high glucose. We confirmed that DGK $\delta$ 2 was immunoprecipitated with the anti-DGK $\delta$  antibody (Fig. 8C). Because the molecular identity of mammalian PC-PLC remains unclear (35), its antibody is unavailable. Therefore, we determined PC-PLC activity in the immunoprecipitates using the Amplex Red<sup>®</sup> PC-PLC assay kit, which detects phosphocholine generated by PC-PLC. As demonstrated in Fig. 8D, PC-PLC activity was clearly co-immunoprecipitated with DGK $\delta$ 2. The assay does not detect the activity of sphingomyelin synthase, which produces DG and sphingomyelin, but not phosphocholine. The contribution of PLD, which hydrolyzes PC to PA and choline, can be accounted for by elimination of alkaline phosphatase from the assay (see “Experimental Procedures”). However, when the assay was performed in the absence of alkaline phosphatase, the activity was not detectable. Taken together, these results strongly suggest that DGK $\delta$ 2 utilizes DG species supplied from PC-PLC-dependent PC hydrolysis in response to high glucose (Fig. 9).

## DISCUSSION

The increase in PA molecular species by stimulation with high glucose levels has not been identified until now. Moreover, it has not been reported that high glucose induces total PA production. The main reasons for this are that PA species are minor components and it is difficult to quantify the amounts of PA molecular species using conventional LC/ESI-MS methods. To overcome this difficulty, we recently established an LC/ESI-MS method specialized for PA species (21). In this study, we revealed for the first time that acute high glucose

## Metabolic Linkage between PC-PLC and DGK $\delta$

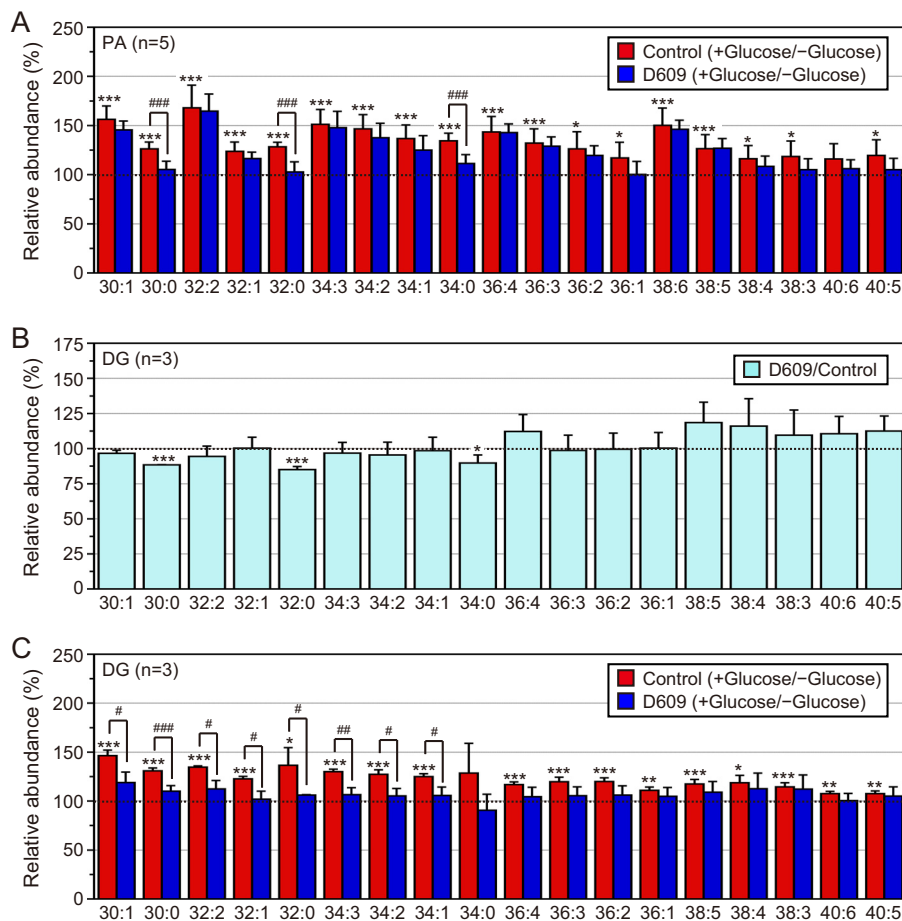


**FIGURE 7. Effect of D609 on high glucose-induced increases in PA and DG molecular species in C2C12 myoblasts.** *A*, the major PA molecular species in the glucose-unstimulated or glucose-stimulated cells treated with DMSO (control) or D609 were detected using the LC/ESI-MS method. The results are presented as the percentage of the value of PA molecular species in glucose-unstimulated cells treated with DMSO (control) or D609. D609 did not significantly affect the value of PA molecular species in glucose-unstimulated cells. The values are presented as the mean  $\pm$  S.D. ( $n = 5$ ). \*,  $p < 0.05$ ; \*\*\*,  $p < 0.005$  (no stimulation versus glucose stimulation). ###,  $p < 0.005$  (without D609 versus with D609). *B* and *C*, the major DG molecular species in the glucose-unstimulated or glucose-stimulated cells treated with DMSO (control) or D609 were detected using the ESI-MS method. *B*, comparison of +D609 versus -D609 in the absence of glucose. The results are presented as the percentage of the value of DG species in glucose-unstimulated cells treated with DMSO (control). The values are presented as the mean  $\pm$  S.D. ( $n = 3$ ). \*,  $p < 0.05$ ; \*\*\*,  $p < 0.005$ . *C*, comparison of +glucose versus -glucose in the absence or presence of D609. The results are presented as the percentage of the value of DG species in glucose-unstimulated cells treated with DMSO (control) or D609. D609 did not significantly affect the value of DG molecular species in glucose-unstimulated cells. The values are presented as the mean  $\pm$  S.D. ( $n = 3$ ). \*,  $p < 0.05$ ; \*\*,  $p < 0.01$ ; \*\*\*,  $p < 0.005$  (no stimulation versus glucose stimulation). #,  $p < 0.05$ ; ##,  $p < 0.01$ ; ###,  $p < 0.005$  (without D609 versus with D609).

stimulation statistically increased the PA mass and number of molecular species using the newly developed method (Fig. 1). The results indicate that our LC/ESI-MS method is a powerful tool for detecting even small changes in PA molecular species.

The suppression of DGK $\delta$  expression by RNA silencing decreased the high glucose-induced production of 30:0-, 32:0-, 34:1-, and 34:0-PA in C2C12 myoblasts (Fig. 2). Moreover, the levels of 30:1-, 30:0-, 32:1-, 32:0-, and 34:0-PA were substantially increased in a high glucose-dependent manner in C2C12 cells stably expressing DGK $\delta$ 2 when compared with control cells (Fig. 4). Taken together, these results strongly suggest that DGK $\delta$  preferentially generates 30:0-, 32:0-, and 34:0-PA, which contain two saturated fatty acids, in the cells. The main fatty acid residues of these PA species were 14:0 and 16:0, 16:0 and 16:0, and 16:0 and 18:0, respectively (Table 1). These results suggest that DGK $\delta$  produces PA with an apparent preference for palmitic acid (16:0)-containing PA. Moreover, the suppression of DGK $\delta$  expression by siRNA-1 and -2 also decreased the high glucose-induced production of 34:1-PA (Fig. 2). The over-

expression of DGK $\delta$ 2 statistically increased the levels of 30:1- and 32:1-PA (Fig. 4). The DGK $\delta$  suppression also modestly attenuated 30:1- and 32:1-PA levels (Fig. 2), and the DGK $\delta$ 2 overexpression slightly augmented 34:1-PA production (Fig. 4). Therefore, it is possible that this enzyme also generates 30:1-, 32:1-, and 34:1-PA, which contain one saturated and one monounsaturated fatty acid, in addition to 30:0-, 32:0-, and 34:0-PA. 30:1-, 32:1-, and 34:1-PA contain saturated fatty acids, 16:0 and 14:0, and monounsaturated fatty acids, 16:1 and 18:1 (Table 1). The DGK $\delta$ -siRNAs and DGK $\delta$  overexpression failed to statistically affect the amounts of high glucose-induced increases of 32:2-, 34:3-, 34:2-, 36:4-, 36:3-, 36:2-, and 38:6-PA (Figs. 2 and 4), implying that these PA species were generated by other DGK isozyme(s).

DGK is a member of the PI turnover pathway and initiates resynthesis of PI (18). This fact led us to believe that DGK isozymes, including DGK $\delta$ , also exhibit selectivity against 38:4 (18:0/20:4)-DG derived from PI turnover. Indeed, it was reported that DGK $\epsilon$  preferentially phosphorylated DGs con-



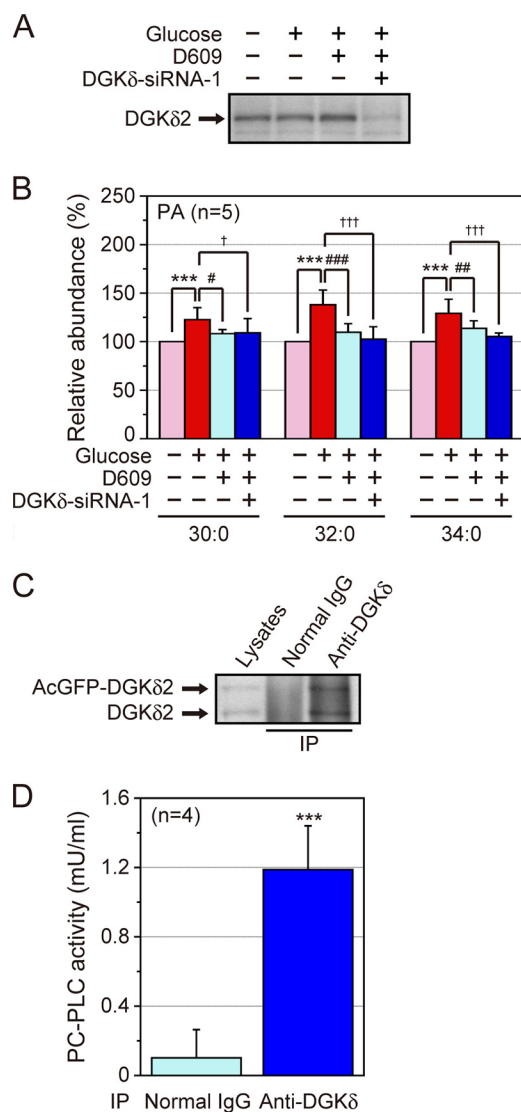


**FIGURE 8. Examination of the functional linkage between PC-PLC and DGK $\delta$ .** Effects of D609 and DGK $\delta$ -siRNA-1 on high glucose-induced increases of PA molecular species in C2C12 myoblasts were compared. *A*, the suppression of DGK $\delta$  expression by DGK $\delta$ -siRNA-1 was confirmed by Western blot analysis using the anti-DGK $\delta$  antibody. *B*, 30:0-, 32:0-, and 34:0-PA in the glucose-unstimulated or glucose-stimulated cells treated with DMSO (control), D609, or D609 and DGK $\delta$ -siRNA-1 were detected using the LC/ESI-MS method. The results are presented as the percentage of the value of PA molecular species in glucose-unstimulated cells. The values are presented as the mean  $\pm$  S.D. ( $n = 5$ ). \*\*\*,  $p < 0.005$  (no stimulation versus glucose stimulation). #,  $p < 0.05$ ; ##,  $p < 0.01$ ; ###,  $p < 0.005$  (without D609 versus with D609). †,  $p < 0.05$ ; †††,  $p < 0.005$  (control siRNA versus DGK $\delta$ -siRNA-1). *C* and *D*, co-immunoprecipitation of PC-PLC activity with DGK $\delta$ . *C*, immunoprecipitation (IP) of DGK $\delta$  using the anti-DGK $\delta$  antibody was confirmed by Western blot analysis using the anti-DGK $\delta$  antibody. *D*, PC-PLC activity in the precipitates was measured using the Amplex Red<sup>®</sup> PC-PLC assay kit. The values are presented as the mean  $\pm$  S.D. ( $n = 4$ ). \*\*\*,  $p < 0.005$ . When the assay was performed in the absence of alkaline phosphatase, the activity was not detectable.

taining arachidonic acid (e.g. 38:4 (18:0/20:4)-DG) derived from PI turnover (7, 19, 20). However, high glucose stimulation did not increase the amount of 38:4-PA (Figs. 1 and 2), which mainly consisted of 18:0/20:4-PA (Table 1). Moreover, DGK $\delta$ -siRNAs and DGK $\delta$  overexpression failed to affect the amounts of 38:4-PA in response to high glucose stimulation (Figs. 2 and 4). These results indicate that DGK $\delta$  does not phos-

phorylate 38:4-DG derived from PI turnover in a glucose-dependent manner.

DGK $\delta$  did not exhibit selectivity against 16:0/16:0 (32:0)- or 16:0/18:1 (34:1)-DG *in vitro* (Fig. 5). Therefore, we hypothesized that DGK $\delta$  exerts substrate selectivity in C2C12 cells through accessing a DG pool containing 30:0-, 32:0-, and 34:0-DG, and not via its intrinsic preference. There are three DG supply pathways, *i.e.* 1) *de novo* synthesis including acetyl-CoA carboxylase (30, 31), 2) the PLD/PA phosphatase route (32), and 3) PC hydrolysis by PC-specific PLC (33). Treatment with the PC-PLC inhibitor D609, but not inhibitors of acetyl-CoA carboxylase and PLD, strongly inhibited the high glucose stimulation-responsive production of 30:0-, 32:0-, and 34:0-PA (Fig. 7A). Moreover, RNA silencing of DGK $\delta$  failed to further inhibit the glucose-dependent increases in 30:0-, 32:0-, and 34:0-PA in the presence of D609 (Fig. 8B). Furthermore, PC-PLC was co-immunoprecipitated with DGK $\delta$  (Fig. 8D). Taken together, these results strongly suggest that 30:0-, 32:0-, and 34:0-DG phosphorylated by DGK $\delta$  in response to acute high glucose exposure are generated, at least in part, by PC hydrolysis catalyzed by PC-PLC (Fig. 9).

The role of sphingomyelin synthase as a potential PC-PLC was indicated (36). We cannot rule out the possibility that DGK $\delta$  partly utilizes sphingomyelin synthase-dependent DG. However, it is likely that DGK $\delta$  phosphorylates DG species generated, at least in part, by PC-PLC because the co-immunoprecipitates with DGK $\delta$  contained PC-PLC activity.

The molecular identity of PC-PLC remains unclear (35). In this study, DGK $\delta$  was revealed to directly or indirectly associate with PC-PLC. With the pull-down of PC-PLC activity with DGK $\delta$ , there may be an opportunity to identify the unidentified PC-PLC enzyme by proteomics approaches. Therefore, DGK $\delta$  may serve as a good tool to search for the PC-PLC molecule.

D609 attenuated high glucose-dependent increases in various C30-C34 DG species (Fig. 7C). However, D609 strongly inhibited only the high glucose stimulation-responsive production of 30:0-, 32:0-, and 34:0-PA (Fig. 7A). Intriguingly, this inhibitor statistically reduced the amounts of 30:0-, 32:0-, and 34:0-DG in the absence of high glucose (Fig. 7B). Therefore, it is likely that, in response to acute high glucose stimulation (5 min), DGK $\delta$  mainly utilizes these DG species supplied from the PC-PLC pathway in a high glucose-independent manner. Moreover, DGK $\delta$  can generate 30:1-, 32:1-, and 34:1-PA, in addition to 30:0-, 32:0-, and 34:0-PA. (Figs. 2 and 4). Although D609 moderately attenuated 30:1-, 32:1-, and 34:1-PA generation (Fig. 7A), this inhibitor did not affect the amounts of 30:1-, 32:1-, and 34:1-DG in the absence of high glucose stimulation (Fig. 7B). However, D609 substantially inhibited high glucose-dependent increases for 30:1-, 32:1-, and 34:1-DG (Fig. 7C). These results suggest that DGK $\delta$  can utilize 30:1-, 32:1-, and 34:1-DG that are supplied from the PC-PLC pathway in a high glucose-dependent manner.

Recently, Shulga *et al.* (37) and Lowe *et al.* (38) reported that DGK $\delta$  positively regulated lipid synthesis, including DG and PA, during adipocyte differentiation. However, unlike for acute high glucose stimulation, a significant preference against DG and PA was not found. The increases were, at least in part, a

## Metabolic Linkage between PC-PLC and DGK $\delta$

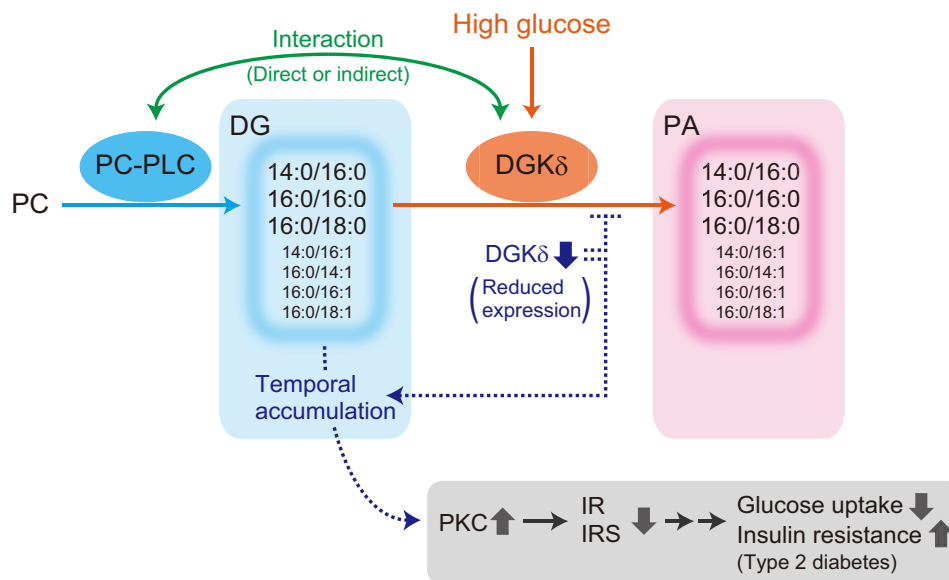


FIGURE 9. Model for the metabolism pathway utilized by DGK $\delta$ . IR, insulin receptor; IRS, insulin receptor substrate.

result of promoting the *de novo* synthesis of fatty acids. However, in this study, an inhibitor of acetyl-CoA carboxylase TOFA did not decrease glucose-stimulated PA production (Fig. 6A). Because differentiation is a long term event, the difference between acute high glucose stimulation in C2C12 myoblasts and adipocyte differentiation may be due to distinct supply pathways and/or fatty acid conversion during long term culture through the remodeling pathway (Lands' cycle) (39).

Chibalin *et al.* (15) previously reported that the transcription of DGK $\delta$  and the levels of DGK $\delta$  protein were also reduced in skeletal muscle from type II diabetes patients. Moreover, in DGK $\delta$  haploinsufficient mice (DGK $\delta^{+/-}$ ), the accumulation of DG, which was caused by decreases in total DGK activity and DGK $\delta$  protein levels in skeletal muscle, increased phosphorylation of PKC $\delta$  and suppressed protein expression of the insulin receptor and insulin receptor substrate-1 for insulin signaling, resulting in the aggravation of type II diabetes (15). Another study reported that the accumulation of DG molecular species with palmitic acid (16:0) is involved in insulin resistance (40). It is generally accepted that saturated fatty acids including palmitic acid induce insulin resistance (41–43). In this study, MS/MS analysis demonstrated that 30:0-, 30:1-, 32:0-, 32:1-, 34:0-, and 34:1-PA commonly contained palmitic acid (16:0), and suggests that DGK $\delta$  mainly consumes 30:0-, 30:1-, 32:0-, 32:1-, 34:0-, and 34:1-DG containing palmitic acid (16:0) supplied from the PC-PLC pathway for glucose uptake in skeletal muscle in a glucose-dependent manner. Acute high glucose- and DGK $\delta$ -dependent increases in 30:0-, 30:1-, 32:0-, 32:1-, 34:0-, and 34:1-PA were relatively minor changes (20–30% increases) when compared with the total amounts of each PA species (Figs. 1 and 2). DGK $\delta$ , which was temporarily activated within 5 min (16), showed a distinct punctate localization pattern in C2C12 cells (17). Therefore, a possible explanation of these findings is that these DGK $\delta$ -dependent minor changes of DG/PA species in temporally and spatially restricted regions play a role in modulating insulin signaling. However, further studies are required to elucidate the relationship between the

specific DG species accumulation in type II diabetes patients and the PC-PLC-DGK $\delta$  pathway disclosed here.

In summary, the present study strongly suggests that DGK $\delta$  preferentially consumes palmitic acid (16:0)-containing DG species such as 30:0-, 30:1-, 32:0-, 32:1-, 34:0-, and 34:1-DG, but not arachidonic acid (20:4)-containing DG species derived from the phosphatidylinositol turnover, in glucose-stimulated C2C12 myoblasts (Fig. 9). Moreover, an unexpected linkage between PC-PLC and DGK $\delta$  emerged. The route “PC  $\rightarrow$  PC-PLC  $\rightarrow$  DG  $\rightarrow$  DGK  $\rightarrow$  PA” proposed here (Fig. 9) is a novel DG metabolic pathway. This new pathway is proposed to play an important role in glucose uptake in skeletal muscle and to be involved in the pathogenesis of type 2 diabetes.

## REFERENCES

- Zimmet, P., Alberti, K. G., and Shaw, J. (2001) Global and societal implications of the diabetes epidemic. *Nature* **414**, 782–787
- Biddinger, S. B., and Kahn, C. R. (2006) From mice to men: insights into the insulin resistance syndromes. *Annu. Rev. Physiol.* **68**, 123–158
- Kraegen, E. W., Saha, A. K., Preston, E., Wilks, D., Hoy, A. J., Cooney, G. J., and Ruderman, N. B. (2006) Increased malonyl-CoA and diacylglycerol content and reduced AMPK activity accompany insulin resistance induced by glucose infusion in muscle and liver of rats. *Am. J. Physiol. Endocrinol. Metab.* **290**, E471–E479
- Goto, K., Hozumi, Y., and Kondo, H. (2006) Diacylglycerol, phosphatidic acid, and the converting enzyme, diacylglycerol kinase, in the nucleus. *Biochim. Biophys. Acta* **1761**, 535–541
- Mérida, I., Avila-Flores, A., and Merino, E. (2008) Diacylglycerol kinases: at the hub of cell signalling. *Biochem. J.* **409**, 1–18
- Sakane, F., Imai, S., Kai, M., Yasuda, S., and Kanoh, H. (2007) Diacylglycerol kinases: why so many of them? *Biochim. Biophys. Acta* **1771**, 793–806
- Shulga, Y. V., Topham, M. K., and Epan, R. M. (2011) Regulation and functions of diacylglycerol kinases. *Chem. Rev.* **111**, 6186–6208
- van Blitterswijk, W. J., and Houssa, B. (2000) Properties and functions of diacylglycerol kinases. *Cell. Signal.* **12**, 595–605
- Sakai, H., and Sakane, F. (2012) Recent progress on type II diacylglycerol kinases: the physiological functions of diacylglycerol kinase  $\delta$ ,  $\eta$  and  $\kappa$  and their involvement in disease. *J. Biochem.* **152**, 397–406
- Sakane, F., Imai, S., Kai, M., Yasuda, S., and Kanoh, H. (2008) Diacylglycerol kinases as emerging potential drug targets for a variety of diseases. *Curr. Drug Targets* **9**, 626–640

11. Sakane, F., Imai, S., Yamada, K., Murakami, T., Tsushima, S., and Kanoh, H. (2002) Alternative splicing of the human diacylglycerol kinase  $\delta$  gene generates two isoforms differing in their expression patterns and in regulatory functions. *J. Biol. Chem.* **277**, 43519–43526
12. Murakami, T., Sakane, F., Imai, S., Houkin, K., and Kanoh, H. (2003) Identification and characterization of two splice variants of human diacylglycerol kinase  $\eta$ . *J. Biol. Chem.* **278**, 34364–34372
13. Sakane, F., Imai, S., Kai, M., Wada, I., and Kanoh, H. (1996) Molecular cloning of a novel diacylglycerol kinase isozyme with a pleckstrin homology domain and a C-terminal tail similar to those of the EPH family of protein tyrosine kinase. *J. Biol. Chem.* **271**, 8394–8401
14. DeFronzo, R. A., Jacot, E., Jequier, E., Maeder, E., Wahren, J., and Felber, J. P. (1981) The effect of insulin on the disposal of intravenous glucose: results from indirect calorimetry and hepatic and femoral venous catheterization. *Diabetes* **30**, 1000–1007
15. Chibalin, A. V., Leng, Y., Vieira, E., Krook, A., Björnholm, M., Long, Y. C., Kotova, O., Zhong, Z., Sakane, F., Steiler, T., Nylén, C., Wang, J., Laakso, M., Topham, M. K., Gilbert, M., Wallberg-Henriksson, H., and Zierath, J. R. (2008) Downregulation of diacylglycerol kinase  $\delta$  contributes to hyperglycemia-induced insulin resistance. *Cell* **132**, 375–386
16. Miele, C., Paturzo, F., Teperino, R., Sakane, F., Fiory, F., Oriente, F., Ungaro, P., Valentino, R., Beguinot, F., and Formisano, P. (2007) Glucose regulates diacylglycerol intracellular levels and protein kinase C activity by modulating diacylglycerol-kinase subcellular localization. *J. Biol. Chem.* **282**, 31835–31843
17. Takeuchi, M., Sakiyama, S., Usuki, T., Sakai, H., and Sakane, F. (2012) Diacylglycerol kinase  $\delta 1$  transiently translocates to the plasma membrane in response to high glucose. *Biochim. Biophys. Acta* **1823**, 2210–2216
18. Hodgkin, M. N., Pettitt, T. R., Martin, A., Michell, R. H., Pemberton, A. J., and Wakelam, M. J. (1998) Diacylglycerols and phosphatidates: which molecular species are intracellular messengers? *Trends Biochem. Sci.* **23**, 200–204
19. Rodriguez de Turco, E. B., Tang, W., Topham, M. K., Sakane, F., Marcheselli, V. L., Chen, C., Taketomi, A., Prescott, S. M., and Bazan, N. G. (2001) Diacylglycerol kinase  $\epsilon$  regulates seizure susceptibility and long-term potentiation through arachidonoyl-inositol lipid signaling. *Proc. Natl. Acad. Sci. U.S.A.* **98**, 4740–4745
20. Tang, W., Bunting, M., Zimmerman, G. A., McIntyre, T. M., and Prescott, S. M. (1996) Molecular cloning of a novel human diacylglycerol kinase highly selective for arachidonate-containing substrates. *J. Biol. Chem.* **271**, 10237–10241
21. Mizuno, S., Sakai, H., Saito, M., Kado, S., and Sakane, F. (2012) Diacylglycerol kinase-dependent formation of phosphatidic acid molecular species during interleukin-2 activation in CTLL-2 T-lymphocytes. *FEBS Open Bio.* **2**, 267–272
22. Amtmann, E. (1996) The antiviral, antitumoural xanthate D609 is a competitive inhibitor of phosphatidylcholine-specific phospholipase C. *Drugs Exp. Clin. Res.* **22**, 287–294
23. Halvorson, D. L., and McCune, S. A. (1984) Inhibition of fatty acid synthesis in isolated adipocytes by 5-(tetradecyloxy)-2-furoic acid. *Lipids* **19**, 851–856
24. Pizer, E. S., Thupari, J., Han, W. F., Pinn, M. L., Chrest, F. J., Frehywot, G. L., Townsend, C. A., and Kuhajda, F. P. (2000) Malonyl-coenzyme-A is a potential mediator of cytotoxicity induced by fatty-acid synthase inhibition in human breast cancer cells and xenografts. *Cancer Res.* **60**, 213–218
25. Su, W., Yeku, O., Olepu, S., Genna, A., Park, J. S., Ren, H., Du, G., Gelb, M. H., Morris, A. J., and Frohman, M. A. (2009) 5-Fluoro-2-indolyl deschlorhalopemide (FIPI), a phospholipase D pharmacological inhibitor that alters cell spreading and inhibits chemotaxis. *Mol. Pharmacol.* **75**, 437–446
26. Bligh, E. G., and Dyer, W. J. (1959) A rapid method of total lipid extraction and purification. *Can. J. Biochem. Physiol.* **37**, 911–917
27. Sakai, H., Tanaka, Y., Tanaka, M., Ban, N., Yamada, K., Matsumura, Y., Watanabe, D., Sasaki, M., Kita, T., and Inagaki, N. (2007) ABCA2 deficiency results in abnormal sphingolipid metabolism in mouse brain. *J. Biol. Chem.* **282**, 19692–19699
28. Callender, H. L., Forrester, J. S., Ivanova, P., Preininger, A., Milne, S., and Brown, H. A. (2007) Quantification of diacylglycerol species from cellular extracts by electrospray ionization mass spectrometry using a linear regression algorithm. *Anal. Chem.* **79**, 263–272
29. Imai, S., Yasuda, S., Kai, M., Kanoh, H., and Sakane, F. (2009) Diacylglycerol kinase  $\delta$  associates with receptor for activated C kinase 1, RACK1. *Biochim. Biophys. Acta* **1791**, 246–253
30. Craven, P. A., Davidson, C. M., and DeRubertis, F. R. (1990) Increase in diacylglycerol mass in isolated glomeruli by glucose from de novo synthesis of glycerolipids. *Diabetes* **39**, 667–674
31. Wolf, B. A., Easom, R. A., McDaniel, M. L., and Turk, J. (1990) Diacylglycerol synthesis *de novo* from glucose by pancreatic islets isolated from rats and humans. *J. Clin. Invest.* **85**, 482–490
32. Bandyopadhyay, G., Sajan, M. P., Kanoh, Y., Standaert, M. L., Quon, M. J., Reed, B. C., Dikic, I., and Farese, R. V. (2001) Glucose activates protein kinase C- $\zeta/\lambda$  through proline-rich tyrosine kinase-2, extracellular signal-regulated kinase, and phospholipase D: a novel mechanism for activating glucose transporter translocation. *J. Biol. Chem.* **276**, 35537–35545
33. Ramana, K. V., Friedrich, B., Tammali, R., West, M. B., Bhatnagar, A., and Srivastava, S. K. (2005) Requirement of aldose reductase for the hyperglycemic activation of protein kinase C and formation of diacylglycerol in vascular smooth muscle cells. *Diabetes* **54**, 818–829
34. Schütze, S., Berkovic, D., Tomsing, O., Unger, C., and Krönke, M. (1991) Tumor necrosis factor induces rapid production of 1'2' diacylglycerol by a phosphatidylcholine-specific phospholipase C. *J. Exp. Med.* **174**, 975–988
35. Adibhatla, R. M., Hatcher, J. F., and Gusain, A. (2012) Tricyclodecan-9-yl-xanthogenate (D609) mechanism of actions: a mini-review of literature. *Neurochem. Res.* **37**, 671–679
36. Luberto, C., and Hannun, Y. A. (1998) Sphingomyelin synthase, a potential regulator of intracellular levels of ceramide and diacylglycerol during SV40 transformation: Does sphingomyelin synthase account for the putative phosphatidylcholine-specific phospholipase C? *J. Biol. Chem.* **273**, 14550–14559
37. Shulga, Y. V., Loukov, D., Ivanova, P. T., Milne, S. B., Myers, D. S., Hatch, G. M., Umeh, G., Jalan, D., Fullerton, M. D., Steinberg, G. R., Topham, M. K., Brown, H. A., and Epan, R. M. (2013) Diacylglycerol kinase  $\delta$  promotes lipogenesis. *Biochemistry* **52**, 7766–7776
38. Lowe, C. E., Zhang, Q., Dennis, R. J., Aubry, E. M., O'Rahilly, S., Wakelam, M. J., and Rochford, J. J. (2013) Knockdown of diacylglycerol kinase  $\delta$  inhibits adipocyte differentiation and alters lipid synthesis. *Obesity* **21**, 1823–1829
39. Shindou, H., Hishikawa, D., Harayama, T., Yuki, K., and Shimizu, T. (2009) Recent progress on acyl CoA:lysophospholipid acyltransferase research. *J. Lipid Res.* **50**, (suppl.) S46–S51
40. Coll, T., Eyre, E., Rodríguez-Calvo, R., Palomer, X., Sánchez, R. M., Merlos, M., Laguna, J. C., and Vázquez-Carrera, M. (2008) Oleate reverses palmitate-induced insulin resistance and inflammation in skeletal muscle cells. *J. Biol. Chem.* **283**, 11107–11116
41. Hu, F. B., van Dam, R. M., and Liu, S. (2001) Diet and risk of Type II diabetes: the role of types of fat and carbohydrate. *Diabetologia* **44**, 805–817
42. Hunicutt, J. W., Hardy, R. W., Williford, J., and McDonald, J. M. (1994) Saturated fatty acid-induced insulin resistance in rat adipocytes. *Diabetes* **43**, 540–545
43. Vessby, B., Uusitupa, M., Hermansen, K., Riccardi, G., Rivellese, A. A., Tapsell, L. C., Näslén, C., Berglund, L., Louheranta, A., Rasmussen, B. M., Calvert, G. D., Maffetone, A., Pedersen, E., Gustafsson, I. B., Storlien, L. H., and KANWU Study (2001) Substituting dietary saturated for monounsaturated fat impairs insulin sensitivity in healthy men and women: the KANWU Study. *Diabetologia* **44**, 312–319